International Journal of Structural Glass and Advanced Materials Research

Original Research Paper

Semi-Probabilistic Calibration of a Partial Material Safety Factor for Structural Silicone Adhesives - Part II: Verification Concept

[1]Michael A. Kraus and [2]Michael Drass

[1]Department of Civil and Environmental Engineering, Stanford University, Y2E2, 473 Via Ortega, Stanford, CA 94305, USA
[2]Institute of Structural Mechancis and Design, Technische Universität Darmstadt, Franziska-Braun-Str. 3, 64287 Darmstadt, Germany

Article history
Received: 11-12-2019
Revised: 28-12-2019
Accepted: 10-01-2020

Corresponding Author:
Michael A. Kraus
Department of Civil and Environmental Engineering, Stanford University, Y2E2, 473 Via Ortega, Stanford, CA 94305, USA
Email: makraus@stanford.edu

Abstract: This paper deals with the application of the semi-probabilistic design concept (level I) to structural silicone sealants where a generally valid verification concept is proposed. The verification concept deals with the classification of silicone adhesive joints into cavitation-insensitive and cavitation-sensitive adhesive joints and at the same time advises which class of material models is necessary for the categorized adhesive joint systems. Furthermore, the static verification of a finite element based limit state analysis is shown within the design verification concept. The concept is elaborated and documented within this paper and illustrated by the help of an example. In the first part of this paper it was found, that the correct level I calibration of that partial material safety factors are significantly lower compared to currently existing estimates and thus allow for a great optimization of structural sealant design situations with potentially high economical as well as sustainability benefits.

Keywords: Partial Material Safety Factor, Structural Silicone, Design and Computation Verification Concept

Introduction and Current Situation

Modern glass façades are designed with a strong emphasis on a transparent appearance with minimal visibility of the supporting structures. In the last fifty years, a lot of experience has been gained worldwide with structural silicone adhesive joints in façade design. Starting with linear adhesive joints, which are used along a window system to ensure homogeneous load transfer (Staudt *et al*., 2018), up to point supported constructions, where glass panes are only glued locally with so-called point fixings (Drass *et al*., 2019a; Santarsiero and Louter, 2019). Recent developments deal with so-called laminated joints, where either a puck is laminated into a Laminated Safety Glass (LSG) or something is hoof laminated onto a glass (Bedon and Santarsiero, 2018).

Although the complexity of adhesive joint applications is increasing, while at the same time there is a desire for a design verification of the sealant joint by means of finite element computations, there is still no generally applicable (and legally formalized) design concept to provide a static verification. Therefore, this paper presents for the first time a generally valid verification concept for silicone adhesive joints in the façade area while simultaneously applying the semi-probabilistic safety concept according to DIN EN 1990 (2010); Drass and Kraus (2019). The aim is to renew the incomprehensible concept of the ETAG 002 (2012), which is based on a global safety factor, by disclosing the mathematical derivation. In order to make the verification concept comprehensible to engineers in practice, a simple design example will be presented within the framework of this paper using the proposed verification concept.

General Methodology for the Verification of Silicone Adhesive Joints

This section proposes a general methodology for the verification of silicone adhesive joints. On the one hand we limit ourselves to ETAG 002-compliant adhesive joints and on the other hand the verification is carried out according to a semi-probabilistic safety concept presented by (Drass and Kraus, 2019). The restriction on ETAG 002-compliant adhesive joints has been

DOI: 10.3844/sgamrsp.2020.10.23

deliberately decided in order to be able to use standard constitutive models for the silicone. In an additional paper to be published by the authors, the verification concept for silicone adhesive joints is extended to any geometry for reasons of clarity.

In the opinion of the authors, a general design verification for silicone adhesive joints using the Finite Element Method (FEM) should be conducted with the following steps:

1. Classification of the Silicone Adhesive Joints
2. Material- and FE Modelling of the Silicone Adhesive
3. Limit State Analysis using the FEM

These three topics are briefly presented below to enable the interested reader to apply the verification concept in relevant façade projects.

In summary, this section is dedicated to the general modelling of silicone adhesive joints in façades and other applications to assist structural engineers in choosing an adhesive joint geometry that directly affects the applicability of constitutive models and the description of failure. First, adhesive joint systems and adhesive geometries from special applications are summarized and special features are discussed. For reasons of clarity, the term "adhesive joint system" will also be used in the following for the applied geometric design of an adhesive joint. In order to objectively categorize the different adhesive joint systems, two criteria from literature are briefly presented and applied to different systems. On this basis, assistance is given for the constitutive description of different systems in order to create a kind of catalogue with regards to adhesive joint systems and the application of corresponding material models. Since the choice of material models is also directly related to the type of adhesive system or adhesive in use, a constitutive model is assigned to each of the various but frequently used adhesives in façade applications. Finally, an example is presented using the DIN EN 1990 (2010) compliant semi-probabilistic safety concept as given by Drass and Kraus (2019), in which the static verification for a real construction project is provided using the finite element method.

Classification of Adhesive Joints

In this section, different adhesive systems, that have already been used in practice, are briefly introduced and classified into cavitation-sensitive and cavitation-insensitive systems using mechanically-motivated and thus objective criteria.

The term '*cavitation-sensitive*' means, that due to the selected geometry ratio of the adhesive joint, it is subjected to volumetric stresses under external loading. This is caused by the obstruction of the lateral contraction and the incompressible material behaviour of the silicone. In order to model this type of deformation and the structural behavior of the adhesive exactly, complex material models describing the volumetric behaviour are necessary (Drass *et al*. 2019a), which however are not considered in further detail in this paper. However, this will be part of an additional paper to come by the authors. Nevertheless, it is necessary to have objective criteria with a mathematical basis in order to be able to decide whether an adhesive joint is likely to show cavitation, i.e., void growth, or whether a joint according to ETAG 002 (2012) is under consideration. This classification means, that in the case of a cavitation-insensitive adhesive joint, deformations occur under almost constant volume. Only cavitation-sensitive adhesive joints will subject the silicone to volumetric loading. At this point, it is important to note that if material models are incorrectly applied to cavitation-sensitive adhesive joints, incorrect verification of the joint may occur, which is potentially on the unsafe side.

The criteria for distinguishing between the two cases are briefly presented below and evaluated for their applicability on typical adhesive bonding systems in the façade sector. The proposed classification makes sense insofar as, for example, the ETAG 002 (2012) concept can be used for cavitation-insensitive adhesive bonding systems as long as the adhesive is linear in its geometry and has only two flanks for bonding. Deviations from ETAG 002 (2012) concept (with its regulated silicone geometries) can only be verified with a significant experimental effort, expert opinions and decision-making boards. In Germany for example, in case of differing from the geometric specifications of adhesive joints according to ETAG 002 (2012), it is possible to verify the ultimate limit state of the adhesive joint using a concept developed at the German Institute for Building Technology (DIBt). This concept is called the DIBt Concept (2012) and requires a wide range of experimental investigations which even exceed the requirements of ETAG 002 (2012). In cases, where neither concept applies, which is the case for flat-sealed point fixings, there still exists no concept for a sensible mechanically and reliability-theoretically correct design verification.

Returning to the classification of silicone adhesive joints, a schematic representation of the classification of typical adhesive bonding systems in façade design is shown in Fig. 1. First of all, a distinction is made between cavitation-sensitive and cavitation-insensitive adhesive joints, while in the last case an additional distinction is made between adhesive joints, which correspond to ETAG 002 (2012) and adhesive joints, which show slight deviations concerning the geometry and requirements according to ETAG 002 (2012).

DOI: 10.3844/sgamrsp.2020.10.23

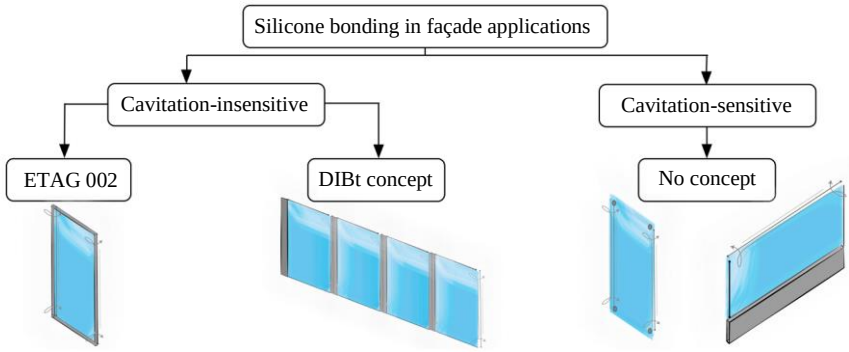

Fig. 1: Schematic classification of adhesive joints for façade applications into cavitation-sensitive and cavitation-insensitive adhesive joints, where the last are subdivided again into adhesive joints according to ETAG 002 (2012) and joints with slight deviations

Criteria for Classification

As already presented by Drass and Kraus (2019), slight geometric deviations of adhesive joints in comparison to the geometry defined in ETAG 002 (2012) require considerable effort in order to provide the proof of structural integrity and safety according to DIBt Concept (2012). To create a clear differentiation between adhesive joints according to ETAG 002 (2012), adhesive joints with slight geometric adjustments or adhesive joints which cannot be verified with any of the mentioned concepts, objective criteria are required to categorise adhesive joints according to their application, external loads and mechanical stresses within the adhesive. The aim is to create a better understanding for structural engineers in order to better design and verify adhesive joints in façade construction.

Accordingly, a criterion must first be found which is capable of clearly distinguish between cavitation-insensitive and cavitation-sensitive adhesive joints. Hamdi *et al*. (2014) have made a suggestion, which is based on the ratio between the diameter d divided by four times the height h of a cylindrical adhesive joint under axial loading. Based on a large test series on so-called pancake tension tests under variation of the shape factor:

$$S = \frac{d}{4h}, \tag{1}$$

cavitation failure was investigated and a critical limit for a cavitation-insensitive geometry of $S \leq 1.0$ (no cavitation) was determined. Since the criterion can only be applied on cylindrical adhesive joint geometries, it will be extended to any geometries in the following. The basic idea of the criterion is to determine the ratio of the surface under tensile stresses to the free surface. Accordingly, it can simply be transferred to the following general form:

$$S = \frac{A}{U\,h}, \tag{2}$$

where, A is the surface area under tensile stress, U represents the perimeter of the adhesive joint and h was already introduced as bondline thickness. Since this geometry factor is a good first approximation to distinguish between cavitation-insensitive and cavitation-sensitive adhesive joints, it is essential to clearly define its limits here as well. Assuming that this criterion was developed from the experimental results of axially loaded pancake tensile tests, it can only be applied to axially loaded adhesive joints. If, for example, one has a very flat adhesive joint that can only be subjected to shear stress due to structural boundary conditions, it is questionable that this type of loading can lead to cavitation failure.

In order to have an improved criterion that can show whether cavitation is relevant for any structure and stress situation of the adhesive joint, the *triaxiality* is introduced. It is a measure to describe the multi-axiality of stresses in any component under any load scenario. Based on the work of Sikora (2014), the triaxiality is defined as the magnitude of the ratio of hydrostatic pressure p = trace(σ) to the von Mises equivalent stress $\sigma_{vM} = \sqrt{3I'_{2,\sigma}}$. For reasons of comprehensibility, this criterion is scaled in a manner to ensure the discrete value of $\eta_{\mathrm{mod}} = 1$ in case of uniaxial tensile loading. Thus, the modified triaxiality reads:

$$\eta_{\mathrm{mod}} = \left| -3\frac{p}{\sigma_{vM}} \right|. \tag{3}$$

Sikora (2014) recommends to extend the discrete, theoretical values of triaxiality to a bandwidth, since single scalar values without upper and lower limits are not realistic boundaries with regards to prevailing stresses and strains in any structural components.

DOI: 10.3844/sgamrsp.2020.10.23

Therefore, Sikora (2014) analysed arbitrary combinations of principal stresses, $\sigma'' = \sigma'' \pm 1/10\sigma''$, where the variation of the Cauchy stress was applied in one or more principal stress directions. With the help of this parameter study, threshold values for uniaxial, biaxial, triaxial and shear deformations could be evaluated (Table 1). At this point it should be noted that these ranges can be individually adapted in case one is interested in stronger or weaker delimitations of deformation processes. In order to decide whether any adhesive joint system is independent of cavitation failure, it is necessary that the triaxiality evaluation does not exceed the critical value of $\eta_{mod} \leq 20$. This means that there is no pronounced volumetric deformation in the material, which excludes excessive void growth and stress softening.

Since this criterion is able to describe the predominant stress state in the sense of multi-axiality for arbitrary adhesive situations and loadings, it is obvious to evaluate and visualize it in the finite element model. Since ANSYS Finite Element (FE) code was used in the course of this work, the procedure for evaluating and visualizing the triaxiality is briefly explained in the following. For this classification of adhesive joints in façade application purpose, a user-defined result must be created in the post-processing after a successful three-dimensional calculation of an adhesive joint has been carried out. The evaluation takes place via principal stresses to which the variables *S*1, *S*2 and *S*3 are assigned in ANSYS FE code. The input file for the user-defined result to evaluate the triaxiality is given by:

```
SUBROUTINE Triaxiality (S1, S2, S3)
eta_mod = abs (2*(S1+S2+S3)
& /(6*((S1)**2 - S1*S2 -S1*S3
& +(S2)**2 - S2*S3+S3 **2)**0.5))*3
END SUBROUTINE
```

Furthermore, a user-defined colour scheme has to be added, where the threshold values are equal to those defined in Table 1.

Examples for Classification

In the previous section, two criteria were presented for classification into cavitation-insensitive and cavitation-sensitive adhesive joint systems. The first criterion is only suitable for axially loaded adhesive joint systems and can be evaluated analytically, cf. (Hamdi *et al*., 2014). The second criterion evaluates the multi-axiality of the three-dimensional stress state in an FE model and thus analyses which deformation states occur in the adhesive as result of external loads (Drass *et al*., 2018a). Now that two criteria are now available for categorizing typical adhesive joint systems used in façades are evaluated below to verify the quality of both criteria.

Table 1: Theoretical and threshold values for modified triaxiality

Stress state	Theoretical value	Modified triaxiality ± 10%
Triaxial	$\eta_{mod} = \infty$	$\infty \geq \eta_{mod} \geq 20$
Biaxial	$\eta_{mod} = 2$	$2.3 \geq \eta_{mod} \geq 1.7$
Uniaxial	$\eta_{mod} = 1$	$1.3 \geq \eta_{mod} \geq 0.72$
Shear	$\eta_{mod} = 0$	$0.17 \geq \eta_{mod} \geq 0$

First of all, the ETAG H-shaped test sample is evaluated because it corresponds to the geometrical boundary conditions according to ETAG 002 (2012) and secondly because it is used to experimentally determine the structural behaviour and (yield) strength for tensile and shear loading. Calculating the shape factor according to Hamdi *et al*. (2014) results in a value of $S = 0.4 < 1.0$, which means that this joint geometry is cavitation-insensitive. The numerical evaluation of the triaxiality of the ETAG H-shaped sample under pure shear loading shows that large areas of the specimen are actually subjected to pure shear loading since $\eta_{mod} < 0.17$. Furthermore, it can be seen from Fig. 2a that no defined deformation state prevails in the marginal areas, since stress superposition occurs here. Finally, it should be noted that according to the criterion of triaxiality, no triaxial stress results, which can also be confirmed by the evaluation of the shape factor according to Hamdi *et al*. (2014). This is proven by the fact that *S* is significantly smaller than one. Therefore, the strict geometrical requirements for adhesive joints according to ETAG 002 (2012) could be made comprehensible on the basis of the presented criteria for distinguishing between cavitation-insensitive and cavitation-sensitive by evaluating the ETAG H-probe.

In the second example, a cantilevered, flat-bonded glass railing system from the Glas Trösch Group is examined with the aforementioned criteria with regards to its susceptibility to cavitation or triaxial stresses. As can be seen in Fig. 2b, it is a cantilevered glass pane, which is flat-bonded in the lower area and functions as a cantilever beam with regard to the fall protection of people. The evaluation of the shape factor *S* of Hamdi *et al*. (2014) results in a value of approx. 4.5, so that this system can be classified as cavitation-sensitive. This can be further proven by the numerical evaluation of the triaxiality, where a triaxial deformation in the centre of the adhesive is clearly visible. Consequently, the standardized design approach according to ETAG 002 (2012) is not applicable for such a system. A prime example of cavitation-sensitive adhesive joints are so-called point fixings, in which large glass panes are connected to the secondary building structure at certain points via thin adhesive joints. As shown as an example in Fig. 2c, the shape factor is $S = 12.5$, which indicates a high risk of cavitation failure. Furthermore, if triaxiality

DOI: 10.3844/sgamrsp.2020.10.23

is evaluated for different stress scenarios, the visual representation quickly shows that large areas in the flat adhesive joint undergo triaxial deformations, so that the cavitation effect is likely to occur. In the last example, a complicated adhesive joint detail is presented, where a U-shaped adhesive joint was formed in a U-steel profile in order to connect glass beams (Hagl, 2016). The evaluation of the shape factor results in a value of 2.5 under axial load, so that cavitation failure is probable. If one continues to evaluate the visual criterion of triaxiality, it becomes clear that large areas also experience triaxial deformations here. As a result, the effect of cavitation is also present in this adhesive joint geometry (cf. Fig. 2d).

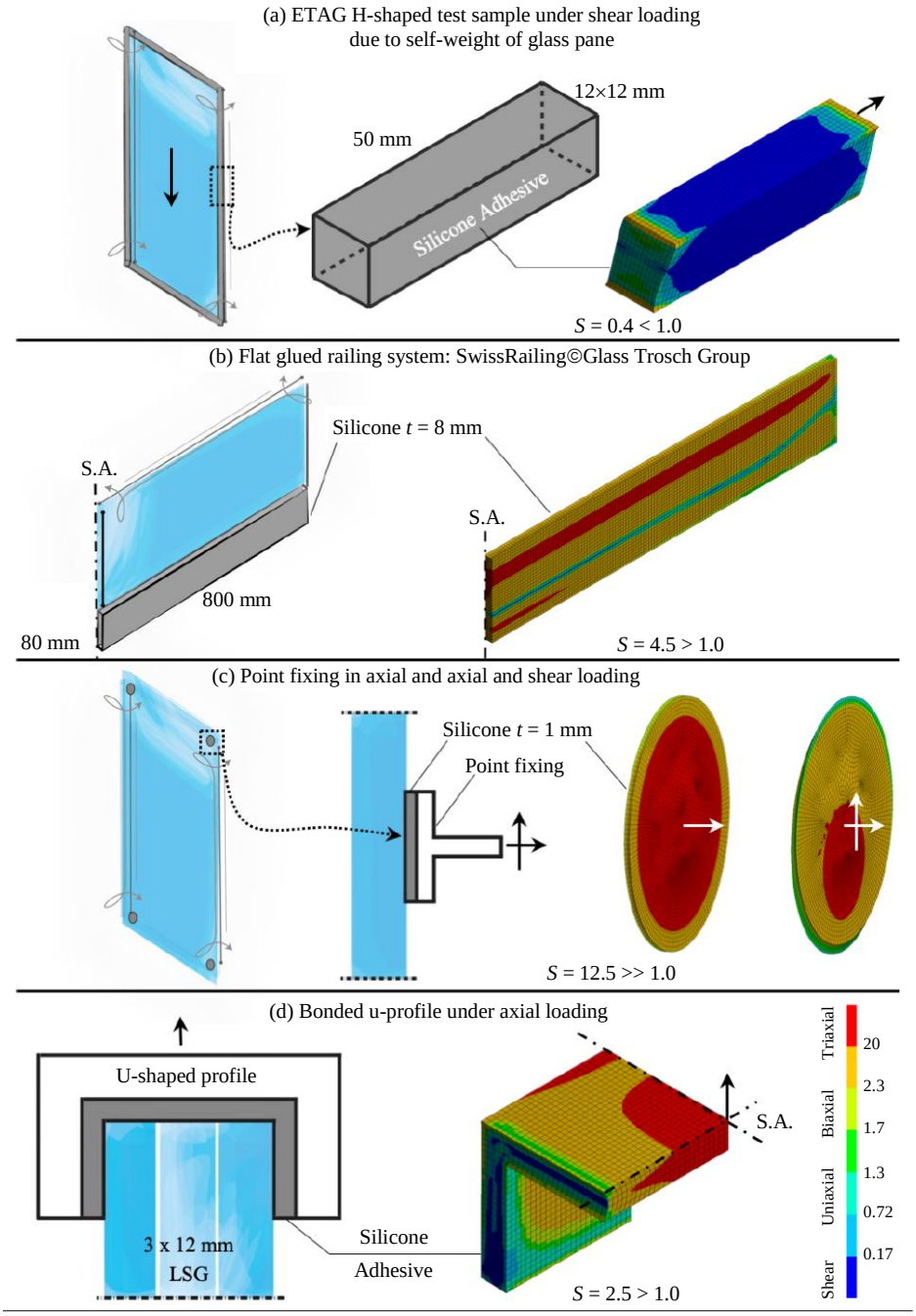

Fig. 2: Numerical evaluation of triaxiality η_{mod} for (a) ETAG H-shaped test sample under shear loading, (b) cantilevered flat-bonded glass railing system under handrail load, (c) point fixing under axial and mixed mode loading and (d) U-shaped bondline for glass beams under axial loading (Hagl 2016)

DOI: 10.3844/sgamrsp.2020.10.23

This descriptive analysis should clearly explain to structural engineers in practice, that the topic of cavitation is an important point when designing adhesive joints in façade applications. Not only in the field of material modelling but also in dimensioning and verification of failure and structural integrity. Considering the stress-based dimensioning of cavitation-sensitive silicone adhesive joints using FE calculations, which are commonly used in façade applications, the calculations lead to large stresses as a result of the triaxial deformation in the core of the material. However, in order to dimension the adhesive joint in accordance with the established technical rules, either the load level is greatly reduced or the global safety factor is adapted to meet the design requirements (Hagl, 2016). Although this procedure leads to the desired result, i.e., the static verification is met, this procedure is mechanically not appropriate and sound since, according to ETAG 002 (2012), a purely isochoric failure is assumed. However, since cavitation-sensitive adhesive joints undergo a triaxial deformation, which is caused in particular by the bulk modulus K and not the shear modulus G for stress calculations, it is not surprising, that high stresses occur in the material even at small external loads and deformations. This can be explained by the fact that in rubber-like materials the bulk modulus K is several orders of magnitudes larger than the shear modulus G due to the silicones being thermomechanically in the entropy-elastic and thus (nearly) incompressible state. Attempting to calculate the structural behaviour cavitation-sensitive adhesive joints and to evaluate the isochoric failure criterion according to ETAG 002 (2012) for volumetric deformations, it is obvious, that the design verification makes no sense on the one hand and is quickly exceeded on the other hand. Therefore, it seems reasonable to categorize the material models for cavitation-insensitive and cavitation-sensitive adhesive joints and to define a separate failure criterion for isochoric and volumetric failure.

Within the scope of this work, however, only cavitation-insensitive joints will be analyzed, as the novel concept for the verification of adhesive joints will be brought closer to the reader step by step. An extension of the concept to cavitation-sensitive adhesive joints becomes part of an additional paper by the authors in near future.

Classification of Material Models

From the categorization of different adhesive connection systems established in practice into cavitation-insensitive and cavitation-sensitive adhesive connections, the influence of the lateral contraction restriction, which can lead to cavitation, has a direct influence on the computation of stresses. Working with wrong assumptions regarding the constitutive model with respect to three-dimensional FE analysis leads to wrong results and incorrect designs of bonded components. Therefore, a recommendation regarding the choice of material models is made in the following in accordance with the categorisation shown in Fig. 1.

Considering first cavitation-insensitive adhesive joint systems, only isochoric, i.e. volume-constant deformations, occur in the material, so that material models implemented in commercially available FE codes can be easily used for stress calculations. Since for typical structural silicones with respect to the façade application, the initial stiffness has to be approximated well in order to perform a robust and physically correct calculation of the occurring stresses (Dispersyn *et al*., 2017), it is recommended to use hyperelastic material models such as the models proposed by Marlow (2003), Dias *et al*. (2014) and Drass *et al*. (2018b). With these material models it has already been shown that the structural response of silicone adhesives can be very well approximated over the entire deformation range. Furthermore, it is recommended to avoid an incompressible material formulation, since on the one hand silicones also allow a slight increase in volume even under isochoric deformations and on the other hand the assumption of incompressibility in numerical calculations may lead to numerical problems and convergence issues during the stress calculation. If, for example, the process of a FE calculation is considered, the condition of $J = 1$ must be enforced via the element technology used (h - p elements). In this context, $J = \det(F)$ means the relative volume change of one finite element. However, this cannot necessarily be guaranteed in all structural situations and calculations. Thus, if the solver allows a supposedly very small increase in volume, the so-called penalty term takes effect, by which the small increase in volume is multiplied by the infinitely large bulk modulus. This may artificially punish the results of the stress computation, as in addition to the stresses from isochoric deformations, stresses are also arising as a result of the penalty term. This may lead to the situation of the static verification is being exceeded when dimensioning an adhesive joint in terms of stresses. If the structural engineer has no experimental data available regarding the bulk modulus, a bulk modulus of approximately $K \approx 1000$ MPa can be assumed as a first approximation for silicone adhesive joints. This results in a deviation between incompressible to compressible material formulations of less than 1% for nearly isochoric deformations while avoiding problem arising from the penalty method.

In contrast, cavitation-sensitive adhesive joint systems must take into account the compressibility due to void growth. As already described by Drass *et al*. (2018c), void growth caused by a triaxial deformation of the material leads to effective stress softening and to large volume changes in the material. Since especially in cavitation-sensitive adhesive joints a triaxial loading of

the material occurs, it is proposed to use the pseudo-elastic cavitation model presented by Drass *et al.* (2019a). This model is characterized by a high quality of adaptation to volumetric experimental data and physically motivated material parameters. The volumetric material parameters for the pseudo-elastic cavitation model to describe the cavitation effect in rubber-like material, here in silicone adhesives, can be determined on the basis of pancake tensile tests and their inverse recalibration. In order to obtain a clear representation for the choice of the material model depending on the adhesive joint geometries to be investigated, reference is made to Fig. 3, in which material models are proposed according to the classification of cavitation-insensitive and cavitation-sensitive adhesive joints.

Limit State Analyses and Safety Concept

In order to verify the adhesive joints in a static design by means of the finite element analysis, a limit state analysis under consideration of a safety concept is necessary. Since we limit ourselves in this paper to ETAG-compliant adhesive joints, we will present generally how the verification concept of ETAG 002 (2012) can be transferred using FEM and further how the semi-probabilistic safety concept according to EC 0 presented in Drass and Kraus (2019) can be applied to the design process. As silicone adhesive the material DOWSIL 993 is examined as an example within this paper.

According to the European Technical Approval (ETA) for DOWSIL 993, the material is allowed a nominal (i.e., engineering stress measure) tensile strength of 0.14 MPa and a nominal shear strength of 0.11 MPa. These nominal design strengths must now be transferred into the context of Finite Element Analysis (FEA). For this purpose, the following two assumptions have to be made or selected in order to be able to perform a verification at all:

- Selection of a suitable material model
- Specification of a predefined FE mesh with a fixed edge length in order to master the problem of stress singularities

To obtain an ETAG 002-compliant failure criterion, the stated design strengths of the investigated structural silicone must be transferred into the context of the FEM. This can be easily done by applying the design failure forces to the ETAG-H specimens in an FE model with a predefined element edge length. When the critical limit force is reached, for example, the true (i.e., Cauchy) principal stress can be obtained. This method is used to transfer the nominal stress according to the ETA of the structural silicone to a true principal stress using FEM $\left(\sigma_{nom}^{des} \rightarrow \sigma_{1,true}^{des}\right)$. It is important that the defined mesh size of the H-specimen corresponds exactly to the mesh size of the structural component. This is necessary to overcome the problem of stress singularities present in any FE solution and influences of the mesh on the magnitude of the obtained stress results. Furthermore, it is important to use a validated constitutive model for this procedure in order to adequately represent the structural behavior of the silicone. The level I approximation of characteristic values for yield tensile and shear stresses with associated partial material safety factors was presented for the DOWSIL 993 in part I of this paper Drass and Kraus (2019).

An exemplary calculation for presentation purposes of the procedure is presented in the example chapter. However, at this point it should be mentioned that any sensible failure criterion can be used and associated with respective partial material safety factors and characteristic values. An important thing thereby is, that failure can adequately be represented by the criterion in comparison to obtained experimental data. However, if one does not want to apply complex failure criteria (as e.g., given in (Drass, 2019; Drass *et al*., 2019b)), one can always access ETAG 002 and apply the criterion presented there.

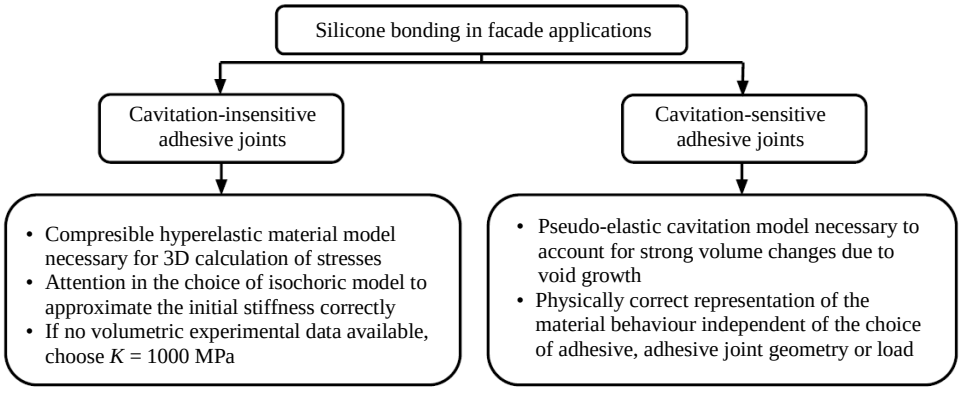

Fig. 3: Engineering toolbox for the schematic classification of adhesive joints for façade applications into cavitation-sensitive and cavitation-insensitive adhesive joints and the recommendation of material models for their modelling or calculation

DOI: 10.3844/sgamrsp.2020.10.23

Verification Example

In this section, a simple example of a glass pane with structural bonding on all sides is calculated and the structural silicone is verified by FEM. The aim of the study is twofold: On the one hand to show how to apply the verification concept in its general form and on the other hand to conduct a comparison of various safety concepts for dimensioning the joint in terms of efficiency and economy. The benchmark problem is described by how much wind load this rectangular plane with silicone adhesive joint support can absorb using different safety concepts. The geometry of the glass pane and the glued joint is therefore defined in advance and the wind load is increased until the ultimate limit state is reached.

Classification

As mentioned above, a glass pane supported by silicone adhesives on all four sides under wind load is to be verified using FEM. The glass pane has a width of a = 1500 mm and a height of b = 3000 mm. The thickness of the glass pane is 10 mm. The adhesive joint is fixed to the edge of the glass pane on all sides. The joint has a width of h_c = 12 mm and a height of e = 6 mm so that the requirements of ETAG 002 (2012) are met, which in detail are:

$$e \le h_c \le 3e \tag{4}$$

and:

$$e \ge 6mm \tag{5}$$

A representation of the system as well as the boundary conditions is shown in Fig. 4. In order to save computational time, only a quarter model was modelled. Accordingly, symmetry conditions were applied to the cut edges. The wind load was defined as external pressure applied to the glass pane. The silicone and the glass were modelled with three-dimensional, higher-order volume elements, whereby the contact between glass and silicone was realized by a so-called internal multipoint constraint (MPC) contact formulation (ANSYS Inc. 2019). The glass was assumed linear elastically with a Young's modulus of E = 70, 000 MPa and a Poisson's ratio of ν = 0.23. The silicone, on the other hand, was initially equipped with a standard compressible Neo-Hookean material model, where the initial shear modulus was chosen to μ = 0.67 MPa and the bulk modulus reads K = 1, 000 MPa. This corresponds to the manufacturer's specifications and allows one to classify the present adhesive joint. At this point where only the classification of the adhesive joint into cavitation-sensitive or insensitive takes place, it is absolutely sufficient to use the compressible Neo-Hooke material model. When performing the structural verification analysis. However, a more accurate constitutive model is used that reproduces the structural behavior of DOWSIL 993 very well. Since a hyperelastic material model is used here a geometrically non-linear calculation was also carried out.

As we have already presented in the section for classification criteria, there are two approaches for the classification of adhesive joints - an analytical approach and a numerical approach. Both are presented in the following example. Evaluating the analytical approach for the present example, one gets a first indication that it is a cavitation-sensitive adhesive joint. So putting the adhesive joint dimensions in Equation (2) results in S = 1.99 ≫ 1.0, so that this criterion says that cavitation may occur in the joint.

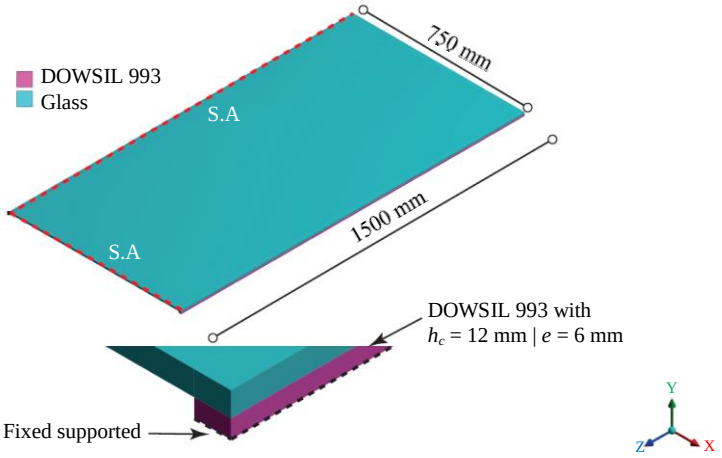

Fig. 4: Glass pane with four-side silicone bonding support under wind load

DOI: 10.3844/sgamrsp.2020.10.23

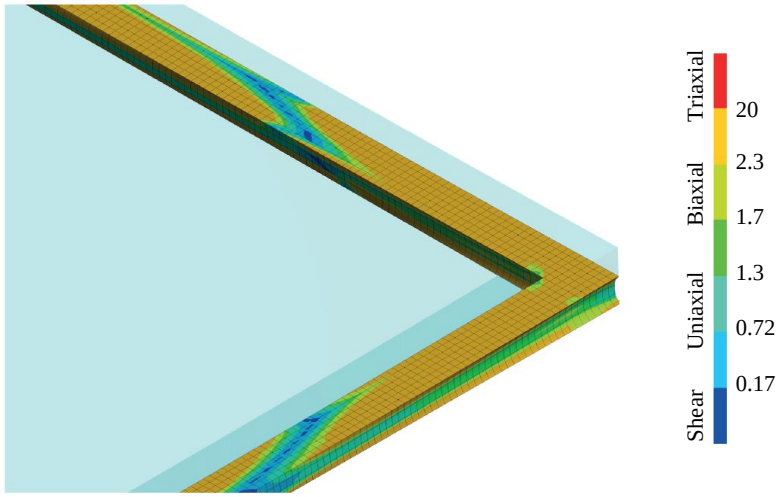

Fig. 5: Evaluation of the triaxiality criterion for the glass pane with four-side silicone bonding support under wind load

In order to study this fact in more detail or to decide whether complex material models have to be applied, the triaxiality proposed in Equation (3) is additionally evaluated numerically in the following in order to better understand the prevailing deformation state of the adhesive joint. Thus, if one carries out this study and evaluates the triaxiality for the silicone, one recognizes that the adhesive joint is mainly utilized by uniaxial or biaxial tension (cf. Fig 5). Triaxial deformations do not occur in the adhesive joint, so that it could be shown that a cavitation-insensitive adhesive joint is present. This means that a standard formulation can be used for the volumetric part of the hyperelastic material model. Since the evaluation of the triaxiality examines the actual deformation condition of the joint much more precisely, this criterion is preferable to the simple manual calculation from Equation (2).

Since the calculation has shown, that a cavitation-insensitive joint is present, the isochoric, i.e. volume constant, part of the hyperelastic material law should be chosen in such a way that it can reproduce the material behaviour of DOWSIL 993 well under any volume constant deformations. This will be shown in the next section. As the volumetric structural behavior is of minor interest, since no triaxial deformation occurs, a standard formulation can be used.

Material- and FE Modelling

In this section, the material modelling for DOWSIL 993 is presented in detail. A novel hyperelastic material model is used, which is ideally suited to represent the strongly non-linear, isochoric material behaviour. Since a cavitation-insensitive adhesive joint is present, the volumetric hyperelastic material model is just equipped with a standard formulation, which will be shown later.

Verification of Material Model

The novel rational Helmholtz free energy function based on the Nelder function (Nelder 1966; Drass, 2019) is applied in the following studies, which is applicable for different types of elastomers and engineering applications. The Helmholtz free energy function consists of four material parameters (α_0, α_1, β_0 and β_1) and all isochoric deformations are described by the first and second isochoric principal invariants:

$$\Psi_{iso} = \frac{\left(I_1 - 3\right)}{\alpha_0 + \alpha_1\left(I_1 - 3\right)} + \frac{\left(I_2 - 3\right)}{\beta_0 + \beta_1\left(I_2 - 3\right)}. \tag{6}$$

As stated above, the volumetric part of the hyperelastic material model is described by a standard linear formulation, which reads:

$$\Psi_{vol} = \frac{K}{2}\left(J - 1\right)^2, \tag{7}$$

where, K represents the bulk modulus of the silicone and J is the relative volume change. Consequently, the complete constitutive law for DOWSIL 993 is as follows:

$$\begin{aligned}\Psi &= \Psi_{iso} + \Psi_{vol} \\ &= \frac{\left(I_1 - 3\right)}{\alpha_0 + \alpha_1\left(I_1 - 3\right)} + \frac{\left(I_2 - 3\right)}{\beta_0 + \beta_1\left(I_2 - 3\right)} + \frac{K}{2}\left(J - 1\right)^2.\end{aligned} \tag{8}$$

As can be seen from Equation (8), five material parameters must be identified for the silicone DOWSIL 993. Without going into detail here, the material parameters are summarized in Table 2 for the structural silicone under consideration, cf. (Drass, 2019).

DOI: 10.3844/sgamrsp.2020.10.23

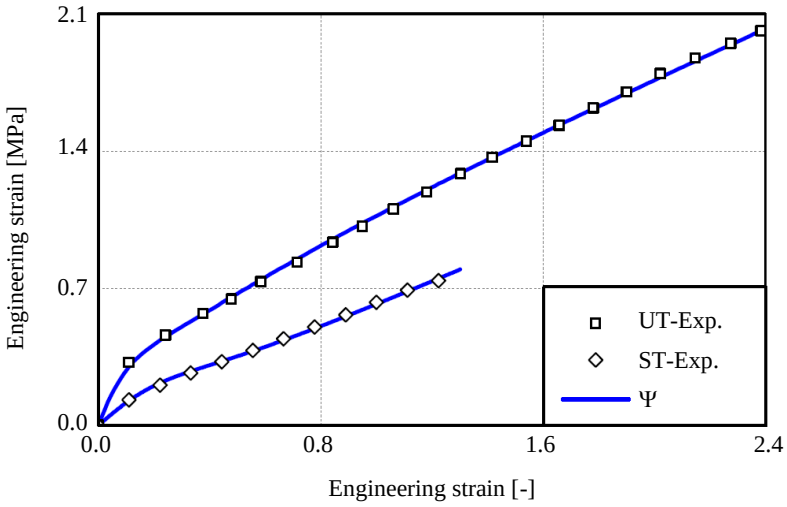

Fig. 6: Fitting results of DOWSIL 993 under Uniaxial Tension loading (UT) and Shear Test (ST)

Table 2: Material parameters of the Helmholtz free energy function Ψ

Model	Parameters	
Isochoric	$\alpha_0 = 3.0127$	$\alpha_1 = 0.0705$
	$\beta_0 = 3.172$	$\beta_1 = 30.129$
Volumetric	$K = 2954$	

The fitting results for a Uniaxial Tensile test (UT) on dogbone test samples and shear tests (ST) for H-shaped test samples are shown in Fig. 6. As it is obvious, the fitting results of DOWSIL 993 under tensile and shear loading while using the novel Helmholtz free energy function presented in 6 show a very good approximation. The structural behavior could thus be very well analytically approximated over the entire deformation range.

Validation of Material Model

Despite the calibration of the material model has shown good fitting result, it is also necessary to validate the material model against experimental data.

To show the quality of the selected material model, the ETAG H-specimen is simulated under tensile loading and compared with experimental data. The classical H-shaped test specimen is commonly used to investigate the structural behavior and failure of silicone adhesives in façade joints. It is made up of steel or glass plates which are connected to each other with a so-called linear adhesive joint (cf. Fig. 7a). In this context, linear means that the adhesive joint is applied linearly along the edges of two components to be joined. The adhesive joint has the dimensions 12×12×50 mm according to ETAG 002 (2012) and is loading uniaxially. In contrast to conventional dumbbell-shaped tensile test specimens, the ETAG test sample exhibits an inhomogeneous stress and strain state, making it ideally suited for the validation of hyperelastic material models.

For validation, the H-sample is numerically analysed in tension, where the material parameters proposed in Table 2 are used as input. A three-dimensional model with higher order element exhibiting quadratic shape functions was set up to avoid numerical locking effects. The numerical model and the results of the validation in the form of force-displacement diagrams are shown in Fig. 7b. Analysing the results of the proposed model, one can conclude that it is capable of accurately reproducing the high initial stiffness. Hence, the new material model allows a good approximation of the global structural behavior of the H-shaped test sample under tensile loading. The high initial stiffness followed by moderate softening can be reproduced very well with the new model. As a result, the validation with the new proposed hyperelastic material model has been successful.

At this point an interesting connection to part I of this paper can be established. In (Drass and Kraus, 2019), the coefficient of variation for the material model V_M was assumed to be 0.10 which can now be quantified for this specific design situation. Within the context of this paper, we follow annex D of EC0 (DIN EN 1990, 2010) to obtain the quality of the resistance model as well as an estimate for the coefficient of variation for the model V_M for predicting the failure load. Taking the data form Fig. 7b, the resistance correction factor can be computed to $b = 0.95$, which means, that the proposed constitutive model on average overestimates experimentally obtained results by 5% (which the resistance model in the following will not be corrected for). Further evaluation of the data result in $V_M = 0.05$ and thus the partial material safety factor γ_M as computed by Drass and Kraus (2019) is a conservative estimation and suitable for the further verification procedure.

DOI: 10.3844/sgamrsp.2020.10.23

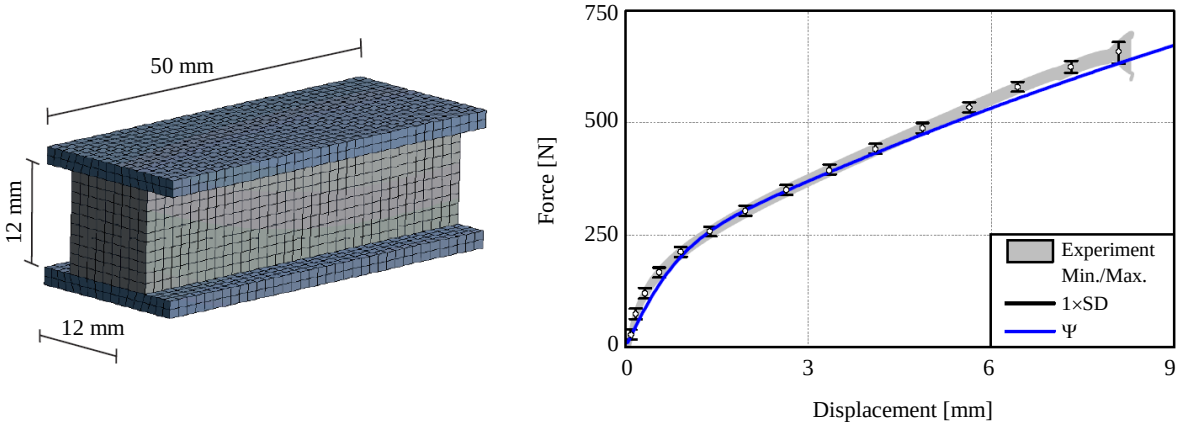

Fig. 7: (a) FE-model of ETAG H-shaped specimen; (b) validation of ETAG H-shaped test sample under uniaxial tensile loading analysing the proposed isochoric hyperelastic material model

Limit State Analyses

In this section the limit state analysis is now carried out using the example of the four-sided supported glass pane under wind load. The support is achieved by linear adhesive joints made of the structural silicone DOWSIL 993. Since the aim is to compare different safety concepts, starting with a global safety concept in accordance with ETAG 002 via a semi-probabilistic partial safety concept in accordance with DIN EN 1990 (2010) (cf. (Drass and Kraus, 2019)), the example is prepared in such a way that the result is the maximum wind load that can be carried in each case, where the higher the design wind load, the more efficient the adhesive joint was dimensioned.

Failure Criterion for DOWSIL 993

To define a failure criterion for DOWSIL 993, first of all a numerical analysis on an ETAG H-specimen with a defined mesh size of 2 mm must be carried out. Since the example analysis a glass pane under wind load, it is sufficient to analyse only the H-sample under tensile load, since the adhesive joint of the structural component is also subjected to tensile load due to the wind load acting on the glass pane. If the component situation nevertheless introduces shear forces into the adhesive joint, this case must also be analysed. However, this is not taken into account in this example.

For this purpose, the ETAG H-specimen must first be simulated under tension using a validated material model. In order to have a direct relationship between FEM and ETAG 002, the H-sample must be loaded with a tensile force defined as:

$$F_{tens} = \sigma_{nom}^{des} \cdot \gamma_{tot} \cdot A = 0.14 \cdot 6 \cdot 12 \cdot 50 = 504N. \quad (9)$$

Since we now have a characteristic load (without any safety level), the results from Equation (9) must be divided by the required safety factor. Applying the semi-probabilistic safety concept according to EC 0, the following loads are specified according to the calculated γ_M from Drass and Kraus (2019), with which the simulations must be carried out. Since in the following example we also apply the concept proposed by ETAG 002 (2012) for reasons of comparison, this load is also defined for the classical global safety concept. A reduced global safety factor of γ_{tot} = 4 acc. to DIBt Concept (2012) is often used in practice when silicone adhesive joints are verified (in Germany) using FEM, however a mathematical background or derivation for this factor is still missing. As this reflects the state of the art, we use in the following the reduced global safety factor of 4.

Looking at Table 3, the FE calculations result in three different true principal stresses, which on the one hand correspond to the reduced ETAG 002 level. On the other hand, the partial safety factor concept according to EC 0 was used to calculate two principal stress values which were computed using the partial material safety factors determined from Drass and Kraus (2019).

Based on the calculated loads, the numerical ETAG H-shaped model is individually loaded with a fixed element size of 2 mm. This size was chosen gratuitously and can be adjusted individually. It is important that the mesh size between ETAG specimen and component is the same in order to circumvent issues related to stress singularities. From the computations, the value of the true principal stress can now be obtained, corresponding to a new true design stress. However, it is important to note that these stress values cannot be directly compared as the ETAG concept as it utilizes a global safety concept to the

DOI: 10.3844/sgamrsp.2020.10.23

resistance side and the EC 0 uses a partial safety concept where safety factors are applied to the action as well as the resistance side. Nevertheless, the following example shows how much wind load this structure can resist given the adhesive joint dimensions.

In order to be able to compute that maximum wind load, the maximum principal stresses in the adhesive joint must be calculated in the FEA and compared with the values of $\sigma_{1,true}^{des}$ in Table 3. The limit state:

$$\sigma_1^{FE} - \sigma_{1,true}^{des} = 0 \tag{10}$$

then provides the maximum wind load that can be carried by the system.

The choice of the principal stress criterion as the limit state function has been deliberately chosen at this point so that the general procedure for the adhesive joint verification is first understood and a direct link to ETAG 002 is provided. In a further paper by the authors it will be shown that instead of Equation (10) any failure criterion can be used as long as it is able to describe the material failure, for example, by a strain or stretch measure (Rosendahl *et al*., 2019).

ETAG 002 - Analytical Approach

Starting with the analytical calculation of the problem, ETAG 002 gives us a hand calculation formula to obtain the maximum design wind load, which acc. to ETAG 002 is computed via:

$$p_{ETAG}^{classic} = \frac{2 \cdot \sigma_{des} \cdot h_c}{a} = \frac{2 \cdot 0.14 \cdot 12}{1500} \cdot 100 = 2.24 \frac{kN}{m^3}. \tag{11}$$

This simple manual calculation represents the current state of the art. However, it should also be noted that the simple verification requires a high global safety factor of 6, since the actual load-bearing behaviour is not represented, nominal stresses are used here and effects due to ageing are not taken into account. Nevertheless, this approach provides an adequately high wind load that the adhesive joint can withstand. Now it has to be shown that with more precise methods it is possible to further increase the wind load that can be carried with that very system in order to justify the additional effort through the FE computation.

Finite Element Computations

This section presents the results of finite element calculations on the four-sided silicone-sealant supported glass pane under wind loading. The mechanical model as well as the material model for the silicone were already presented in the prior sections.

In the computations carried out, the wind load was thus increased until the respective failure criterion was reached. The failure criterion, which must be evaluated in the FEA is already defined in Equation (10). The corresponding principal failure stresses in accordance with the particularly chosen safety concept are given in Table 3. At this point it is important to note that these design stresses are tied to the FE mesh with an edge length of 2 mm. Therefore, the calculations of the silicone adhesive joint of the glass pane with an edge length of 2 mm must also be performed. As a reminder, the ETAG 002 concept was transferred to the FEM using different global safety factors and the semi-probabilistic safety concept according to EC 0 for the DOWSIL 993 was developed and applied.

After successful calculation, the silicone is checked to see if the critical, true principal stress has been reached. The corresponding wind load is then obtained. For better illustration, a deformation plot of the quarter model is shown in Fig. 8. The maximum wind loads for the different safety concepts are summarized in Table 4. In order to have comparability between global and semi-probabilistic safety concepts, the wind loads determined for the semi-probabilistic safety concept must be divided by the partial safety factor from the action side. Since we only consider wind loads in this example, the determined wind load is divided by γ_{Ed} = 1.5. The adjusted values are shown directly in Table 4, so that the levels of the calculated wind loads can be directly compared on their characteristic level.

Table 3: Critical, true principal stress for DOWSIL 993 for different safety concepts

	ETAG 002 (2012)-red	PSF-A	PSF-B
Safety Factor	γ_{tot} = 4	γ_M, 5% = 1.63	γ_M,10% = 2.02
Force [N]	$F_{\mathrm{ETAG,red}}$ = 126	$F_{\mathrm{PSF-A}}$ = 309	$F_{\mathrm{PSF-B}}$ = 250
$\sigma_{1,true}^{des}$ [MPa]	0.64	1.43	1.16

Table 4: Maximum characteristic wind load of the system for different safety concepts

	ETAG-Manual	ETAG-FEM	PSF-A	PSF-B
Safety Factor	γ_{tot} = 6	γ_{tot} = 4	γ_{M}, 5% = 1.63	γ_{M}, 10% = 2.02
pk [kN/m^2]	2.24	1.51	3.59	2.59

DOI: 10.3844/sgamrsp.2020.10.23

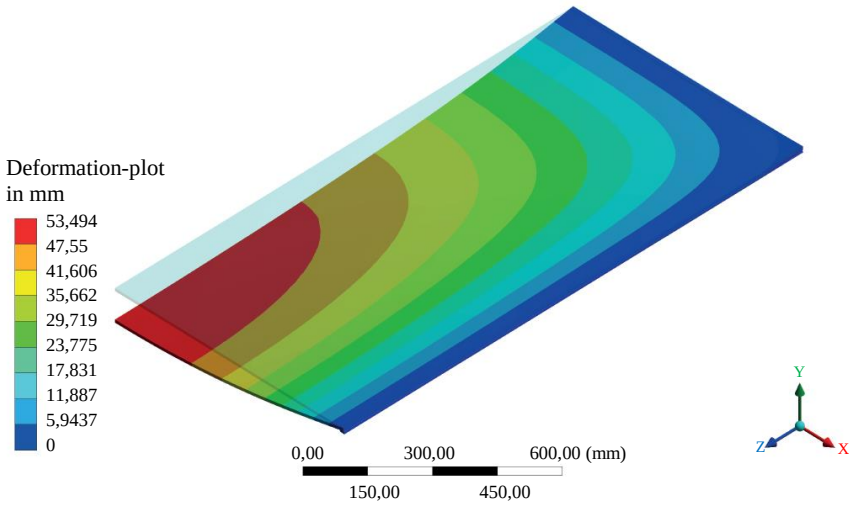

Fig. 8: Deformation plot of a four-sided, glued glass pane under a wind load of p = 10 kN/m^2

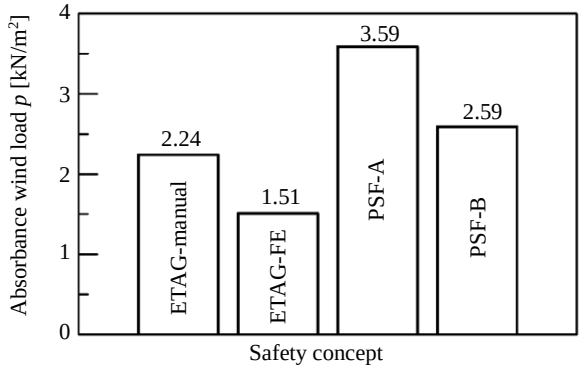

Fig. 9: Histogram of permissible wind loads with respect to the chosen safety concept

Discussion

Comparing the results from Table 4, it is interesting, that the FE simulation with safety factor of 4 delivers a 33% lower wind load than the analytical solution acc. to ETAG 002. This can be justified by the fact that in the FE simulation the state of deformation within the adhesive joint is described much more precisely and no 'smeared' nominal stresses are evaluated. Despite the adjustment of the global safety factor from 6 to 4 as a result of the exact calculation, this method nevertheless provides a conservative result compared to the analytical solution. Furthermore, one can also argue the opposite way and claim that the assumptions made in the manual calculation according to ETAG 002 represent the actual structural behavior very inaccurately. Although one tries to counteract these inaccuracies with the global safety factor of 6, it was shown here, that one cannot say with certainty whether this level is sufficient at all. From the literature, many sources are known that trust the safety level of 6, but an exact derivation of the safety factor was never published.

Comparing the results from the semi-probabilistic with the global safety concept, the wind load could be significantly increased compared to the manual calculation (Fig. 9) by an exact FEM simulation together with specifically and consistently derived partial material safety factors. For the assumed case of having model and geometry coefficients of variation of 10%, resulting in a γ_M = 2.02 as proposed by Drass and Kraus (2019), a load increase of 16% is seen. If these variabilities could be reduced to 5%, the wind load can further be increased by 61% compared to manual calculation. This represents a significant progress, since not only loads could be increased, but also a mathematical basis for determining a partial material safety factor was presented and applied to the structural silicone DOWSIL 993 for a stress based failure criterion. Finally, within this paper it was shown how a verification concept can be methodically carried out using FEM.

To this end, the two parts of this publication have high significance for both, scientific as well as practical aspects of a Eurocode-conform and state-of-the-art design and verification process for structural silicones.

Conclusion

In this paper a mechanistic and thus generally valid verification concept for the dimensioning of silicone adhesive joints with the FEM was presented. With the help of this concept, it is now possible to numerically accurately verify complex adhesive structures. Furthermore, the Eurocode-compliant semi-probabilistic safety concept for a silicone (DOWSIL 993) was presented and applied for the first time in the verification concept. Here, it could be shown in a very

simple example that load bearing reserves can be exhausted without saving on safety. It could also be shown that with the mathematically founded basis of the partial safety factor for silicone, adhesive joints can for the first time be calculated and evaluated on the basis of the Eurocode. This is a novelty and has not yet been carried out. Furthermore, by deriving a partial safety factor for silicone, the discussion about the global partial safety factor according to ETAG 002 can finally be silenced, as a comprehensible derivation has now been given for the first time.

Author's Contributions

The authors contributed equally to this work.

Ethics

This article is original and contains unpublished material. The corresponding author confirms that all of the other authors have read and approved the manuscript and no ethical issues involved.

References

Bedon, C. and M. Santarsiero, 2018. Transparency in structural glass systems via mechanical, adhesive and laminated connections - existing research and developments. Adv. Eng. Mater., 20: 1700815-1700815. DOI: 10.1002/adem.201700815

Dias, V., C. Odenbreit, O. Hechler, F. Scholzen and T.B. Zineb, 2014. Development of a constitutive hyperelastic material law for numerical simulations of adhesive steelglass connections using structural silicone. Int. J. Adhesion Adhesives, 48: 194-209. DOI: 10.1016/j.ijadhadh.2013.09.043

DIBt Concept, 2012. Vorschlag: Zeitstandnachweis für geklebte lastabtragende Verbindungen.

DIN EN 1990, 2010. Eurocode: Grundlagen der tragwerksplanung. Deutsche Fassung EN 1990: 2002+ Al: 2005+ A1: 2005/AC.

Dispersyn, J., S. Hertelé, W.D. Waele and J. Belis, 2017. Assessment of hyperelastic material models for the application of adhesive point-fixings between glass and metal. Int. J. Adhesion Adhesives, 77: 102-117. DOI: 10.1016/j.ijadhadh.2017.03.017

Drass, M., 2019. Constitutive modelling and failure prediction of silicone adhesives in facade design. PhD Thesis, Technische Universität Darmstadt.

Drass, M. and M.A. Kraus, 2019. Semi-probabilistic calibration of a partial material safety factor for structural silicone adhesives. Engineering Structures.

Drass, M., G. Schwind, J. Schneider and S. Kolling, 2018a. Adhesive connections in glass structures-part I: Experiments and analytics on thin structural silicone. Glass Struct. Eng., 3: 39-54. DOI: 10.1007/s40940-017-0046-5

Drass, M., G. Schwind, J. Schneider and S. Kolling, 2018b. Adhesive connections in glass structures-part II: Material parameter identification on thin structural silicone. Glass Struct. Eng., 3: 55-74. DOI: 10.1007/s40940-017-0048-3

Drass, M., J. Schneider and S. Kolling, 2018c. Novel volumetric Helmholtz free energy function accounting for isotropic cavitation at finite strains. Mater. Design, 138: 71-89. DOI: 10.1016/j.matdes.2017.10.059

Drass, M., P.A. Du Bois, J. Schneider and S. Kolling, 2019a. Pseudo-elastic cavitation model-Part I: Finite element analyses on thin silicone adhesives in Façades. Glass Structures Eng.

Drass, M., P. Rosendahl, M.A. Kraus, V.A. Kolupaev and J. Schneider *et al*., 2019b. Coupled distortional-dilatational failure mode concept for rubber-like materials. Constr. Build. Mater.

ETAG 002, 2012. Guideline for European technical approval for structural SealantGlazing Kits.

Hagl, A., 2016. Development and test logics for structural silicone bonding design and sizing. Glass Struct. Eng., 1: 131-151. DOI: 10.1007/s40940-016-0014-5

Hamdi, A., S. Guessasma and M.N. Abdelaziz, 2014. Fracture of elastomers by cavitation. Mater. Design, 53: 497-503. DOI: 10.1016/j.matdes.2013.06.058

Marlow, R., 2003. A general first-invariant hyperelastic constitutive model. Proceedings of the 3rd European Conference on Constitutive Models for Rubber, (CMR' 03), London, pp: 157-160.

Nelder, J.A. 1966. Inverse polynomials, a useful group of multifactor response functions. Biometrics, 22: 128-141. DOI: 10.2307/2528220

Rosendahl, P.L., M. Drass, J. Felger, J. Schneider and W. Becker, 2019. Equivalent strain failure criterion for multiaxially loaded incompressible hyperelastic elastomers. Int. J. Solids Struct., 166: 32-46. DOI: 10.1016/j.ijsolstr.2019.01.030

Santarsiero, M. and C. Louter, 2019. Metal-to-Glass Bond Strength of Structural PVB. Proceedings of the GPD Glass Performance Days, (GPD' 19).

Sikora, S.P., 2014. Materialcharakterisierung und-modellierung zur Simulation von Klebverbindungen mit Polyurethanklebstoffen. PhD Thesis, Universität Paderborn.

Staudt, Y., C. Odenbreit and J. Schneider, 2018. Failure behaviour of silicone adhesive in bonded connections with simple geometry. Int. J. Adhesion Adhesives, 82: 126-138. DOI: 10.1016/j.ijadhadh.2017.12.015